Title

Electronic Effects of Bidentate P,N-Ligands on the Elementary Steps of Au(I)/Au(III) Reactions Relevant to Cross-Coupling Chemistry.

Journal

Organic Letters, 26(50)

Authors

Treacy, Joseph
Chao, Elaine
Kunkel, Grace
et al.

Publication Date

2024-12-20

DOI

10.1021/acs.orglett.4c04045

Peer reviewed

OL Organic Letters

pubs.acs.org/OrgLett

Letter

Electronic Effects of Bidentate *P,N*-Ligands on the Elementary Steps of Au(I)/Au(III) Reactions Relevant to Cross-Coupling Chemistry

Joseph W. Treacy,‡ Elaine Y. Chao,‡ Grace E. Kunkel, Thomas Louis-Goff, James A. R. Tilden, Alexander M. Spokoyny,* Heather D. Maynard,* and K. N. Houk*

Cite This: *Org. Lett.* 2024, 26, 10875−10879

Read Online

ACCESS | Metrics & More | Article Recommendations | Supporting Information

ABSTRACT: Oxidant-free Au(I)/Au(III)-catalyzed cross-coupling has been recently enabled by the use of bidentate *P,N*-ligands. To further develop these *P,N*-ligands, computational studies were performed to understand their effects on the oxidative addition of aryl iodide electrophiles with Au(I). Using this mechanistic understanding, six new electron-rich *P,N*-ligands were synthesized. The ligand exchange equilibrium and reductive elimination were then characterized by using a Au(III)-mediated *S*-arylation reaction. The results detailed herein provide new fundamental insights in Au(I)/Au(III) ligand design.

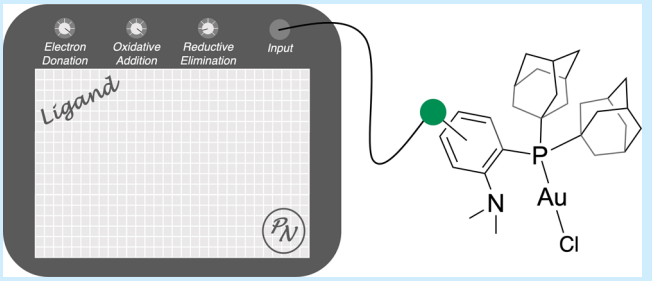

The advent of oxidant-free Au(I)/Au(III) redox catalysis has been enabled by careful ligand choice to provide an alternative to well-defined, two-electron Pd(0)/Pd(II) redox catalysis despite the higher redox potential of Au(I)/Au(III) compared to that of Pd(0)/Pd(II) ($E°$ = 1.41 to 0.92 V, respectively).[1] Most notably, the hemilabile bidentate *P,P*- and *P,N*-ligands have recently received significant attention due to their ability to stabilize the Au(III) center.[2−7] Other *C,N*-ligands have also been investigated to mediate these transformations[8,9] along with tridentate, pyridyl-based species.[10,11] These ligated Au(I)/Au(III) complexes have been used for the catalytic construction of $C(sp^2)-C(sp^2)$,[3,12,13] $C(sp^2)-N$,[14−16] $C(sp^2)-O$,[17,18] $C(sp^2)-Se$,[19] $C(sp^2)-S$,[4,19,20] and $C(sp^2)-C(sp^3)$ bond formation.[21] Modification of the hemilabile *P,N*-ligand to incorporate chirality has also generated platforms for enantioselective transformations.[22,23] Generally, these catalytic methods use a *P,N*-ligated Au(I) precatalyst, often (Me-DalPhos)AuCl, in the presence of a silver salt and base to enable these valuable transformations.

In order to further develop new and/or improved reactivity, it is critical to understand the role of the ligand with regard to each elementary step of the reaction cycle. Recently, our groups reported the use of stopped-flow/UV−vis spectroscopy to monitor the rates of the ligand exchange and reductive elimination for Au(III)-mediated *S*-arylation.[24] This mechanistic insight led to the development of a sterically less bulky *P,N*-ligand that improved the rate of thiol coordination to the Au(III) center from 2,560 to 16,600 M^{-1} s^{-1}. However, the less bulky ligand slowed the reductive elimination from 7.92 to 1.28 s^{-1}, highlighting the opposing effect on rates for these elementary steps. While these steric effects were examined for the ligand exchange and reductive elimination, they were not determined for the oxidative addition, which is often the limiting step in these reactions. Moreover, no elucidation of the ligand's electronic effects on any of the elementary organometallic steps was performed.

To determine the effects of the *P,N*-ligand on the rate of oxidative addition with Au(I) species, the reaction for the oxidative addition of iodobenzene with *P,N*-ligated Au(I) reagents was computed. The proposed mechanism begins with halide abstraction by $AgSbF_6$ to form a cationic gold species with the SbF_6^- counteranion (*SM*). Subsequent coordination of the iodoarene forms the iodine-coordinated intermediate (*Int1*) that undergoes a formal oxidative addition generating the Au(III) complex (*P*).[3] By modulation of the amine and diphosphine components of the ligand, one can examine their effects on the oxidative addition barrier. Initially, the free-energy diagrams were computed with di-1-adamantylphosphine (**1**, PAd_2), di-*tert*-butylphosphine (**2**, P^tBu_2), and dicyclohexylphosphine (**3**, PCy_2) *P,N*-ligated Au complexes with a dimethylamino group as the *N*-substituent at the ωB97X-D/6-311+G(d,p), SDD, SMD(dichloromethane)//B3LYP-D3/6-31G(d), LANL2DZ, and SMD(dichloromethane) level of theory. Despite having significantly different steric profiles, these ligands have very similar free energies of activation (16.4−18.2 kcal/mol, Figure 1A) for oxidative addition ($\Delta G_{OA}^{\ddagger}$), suggesting that this reaction may be driven primarily by the electronic effects of the *P,N*-ligand. To test this hypothesis, calculations were

Received: October 27, 2024
Revised: December 3, 2024
Accepted: December 5, 2024
Published: December 9, 2024

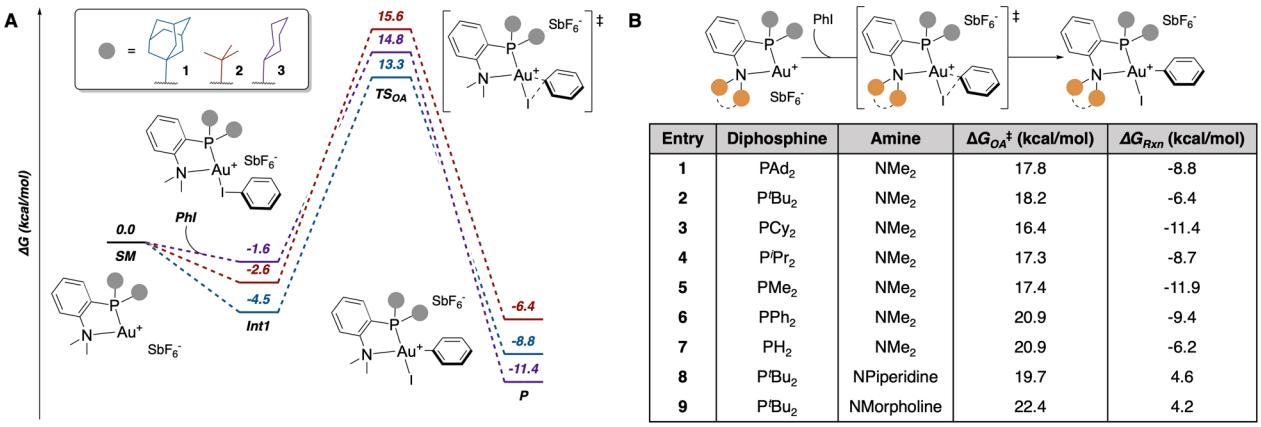

Entry	Diphosphine	Amine	$\Delta G_{OA}^{\ddagger}$ (kcal/mol)	ΔG_{Rxn} (kcal/mol)
1	PAd_2	NMe_2	17.8	-8.8
2	P^tBu_2	NMe_2	18.2	-6.4
3	PCy_2	NMe_2	16.4	-11.4
4	P^iPr_2	NMe_2	17.3	-8.7
5	PMe_2	NMe_2	17.4	-11.9
6	PPh_2	NMe_2	20.9	-9.4
7	PH_2	NMe_2	20.9	-6.2
8	P^tBu_2	NPiperidine	19.7	4.6
9	P^tBu_2	NMorpholine	22.4	4.2

Figure 1. A) Reaction coordinate diagrams for the oxidative addition of iodobenzene with PAd_2- (**1**), P^tBu_2- (**2**), and PCy_2-based (**3**) *P,N*-ligated Au(I) complexes calculated at the ωB97X-D/6-311+G(d,p), SDD, SMD(dichloromethane)//B3LYP-D3/6-31G(d), LANL2DZ, SMD-(dichloromethane) level of theory. B) Calculated $\Delta G_{OA}^{\ddagger}$ and ΔG_{Rxn} for the oxidative addition of iodobenzene with different diphosphine and amine substituents on the *P,N*-ligated Au complex.

performed with smaller dialkylphosphine *P*-substituents, namely, diisopropylphosphine (**4**, P^iPr_2) and dimethylphosphine (**5**, PMe_2), which had $\Delta G_{OA}^{\ddagger}$ values of 17.3 and 17.4 kcal/mol, respectively (Figure 1B). This confirms that there is little steric dependence of the diphosphine substituent on the $\Delta G_{OA}^{\ddagger}$. By examining more electron-deficient diphosphine substituents on the *P,N*-ligand scaffold, namely, diphenylphosphine (**6**, PPh_2) and dihydrophosphine (**7**, PH_2), a $\Delta\Delta G_{OA}^{\ddagger}$ of >2.7 kcal/mol for **6** and **7** compared to **1**−**5** was observed. Furthermore, the *N*-substituent was varied as other DalPhos ligands have been shown to induce valuable catalytic transformations.[14,25−30] In agreement with the calculations for the diphosphine-modified *P,N*-ligands, the more electron-deficient amines, piperidine (**8**) and morpholine (**9**),[31,32] have higher $\Delta G_{OA}^{\ddagger}$ values of 19.7 and 22.4 kcal/mol, respectively. Notably, the free energy of reaction (ΔG_{Rxn}) is endergonic for the **8** and **9** ligated complexes, likely due to the less donating amine poorly stabilizing the cationic Au center. For each dimethylamino-substituted *P,N*-ligated complex (**1**−**7**), ΔG_{Rxn} is exergonic and the equilibrium favors the formation of the Au(III) oxidative addition complex (*P*). Taken together, these results demonstrate that while there is no observable steric effect significantly influencing the oxidative addition barrier, more electron-rich ligands do lower the $\Delta G_{OA}^{\ddagger}$ and vice versa (Figure 1B).

In order to improve the kinetics of the oxidative addition for *P,N*-ligated Au(I) complexes, we sought to add electron-donating groups to the aryl rings both *para* and *meta* to the *N*-substituent (Figure 2). Accordingly, the effects of methyl, methoxy, and dimethylamino substituents were computationally examined as weak, mild, and strong electron donating groups, respectively.[33] When these substituents are *para* to the *N*-substituent, there is no change ($\Delta\Delta G_{OA}^{\ddagger}$ < −0.4 kcal/mol) for both the methyl (**10**) and methoxy (**11**) groups compared to the unsubstituted ligand (**1**). However, with the dimethylamino substituent (**12**), there is a $\Delta\Delta G_{OA}^{\ddagger}$ of −1.7 kcal/mol compared to that of **1**. These minimal changes for **10** and **11** are likely due to the nitrogen of the *P,N*-ligand being out of the plane of the ring and being unable to effectively receive electronic donation from the added substituents. When the substituents are *meta* to the amine, more significant decreases in $\Delta G_{OA}^{\ddagger}$ for the methyl substituent (**13**, $\Delta G_{OA}^{\ddagger}$ = 15.4 kcal/mol) are observed, likely due to the increased donating capacity of the substituent to the phosphorus of the *P,N*-ligand.[33] However, there is no change with the methoxy substituent (**14**, $\Delta G_{OA}^{\ddagger}$ = 17.8 kcal/mol). We propose that this is due to the ability of the methoxy substituent to act as both an inductively withdrawing group and a resonance donating group, which counteract any effects that would lead to a change in $\Delta G_{OA}^{\ddagger}$. With the electron-rich dimethylamino substituent (**15**), a $\Delta G_{OA}^{\ddagger}$ value of 13.7 kcal/mol was calculated. This value is 4.1 kcal/mol lower than that of **1**, further emphasizing the ability of electronic effects to modulate the oxidative addition barrier (Figure 2).

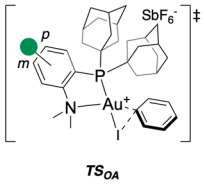

Entry	Substituent	$\Delta G_{OA}^{\ddagger}$ (kcal/mol)
1	H	17.8
10	*p*-Me	17.4
11	*p*-OMe	17.7
12	*p*-NMe_2	16.1
13	*m*-Me	15.4
14	*m*-OMe	17.8
15	*m*-NMe_2	13.7

Figure 2. Calculated $\Delta G_{OA}^{\ddagger}$ for the oxidative addition of iodobenzene with aryl substituents at the *p*- or *m*-site on the *P,N*-ligated Au complex.

Given that the aforementioned aryl modifications show either no change or a decrease in the oxidative addition barrier (Figure 2), we sought to synthesize these ligands and their corresponding Au(I) complexes and Au(III) oxidative addition complexes (OACs) to examine their reactivity in the ligand exchange and reductive elimination. To prepare these Au(III) compounds, the *P,N*-ligands were synthesized via Pd-catalyzed C(sp^2)-*P* cross-coupling with di-1-adamantylphosphine from the *ortho*-halo-dimethylaniline. These ligands were then metalated to access the Au(I) complex. Oxidative addition with Au(I), a silver salt, and an aryl iodide generated the Au(III) OAC (Figure 3A). *P,N*-Ligands containing *p*-methyl (**16**), *p*-methoxy (**17**), and *p*-dimethylamino (**18**) substituents relative to the aniline were synthesized in 56−68% yield, and the ligands containing *m*-methyl (**19**), *m*-methoxy (**20**), and *m*-dimethylamino (**21**) substituents relative to the aniline were isolated in 57−84% yield (Figure 3B, see the SI for details). Notably, all ligands were isolated by flash column chromatography, and most can be stored under open air conditions with no appreciable formation of the phosphine oxide for months. However, **21** showed some degradation to the phosphine oxide product over

https://doi.org/10.1021/acs.orglett.4c04045
Org. Lett. 2024, 26, 10875−10879

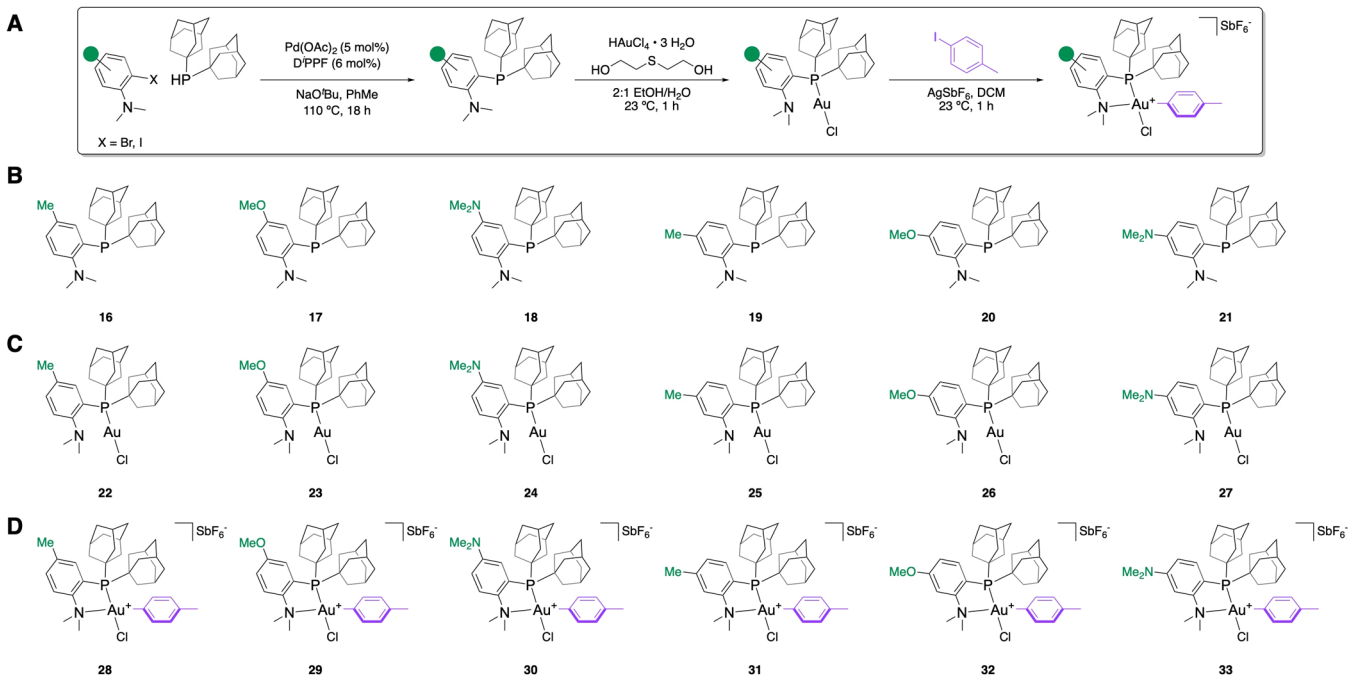

Figure 3. A) General scheme to synthesize *P,N*-ligands, Au(I) complexes, and Au(III) OACs. B) Structures of electron-rich *P,N*-ligands synthesized. C) Structures of Au(I) complexes synthesized. D) Structures of Au(III) OACs synthesized.

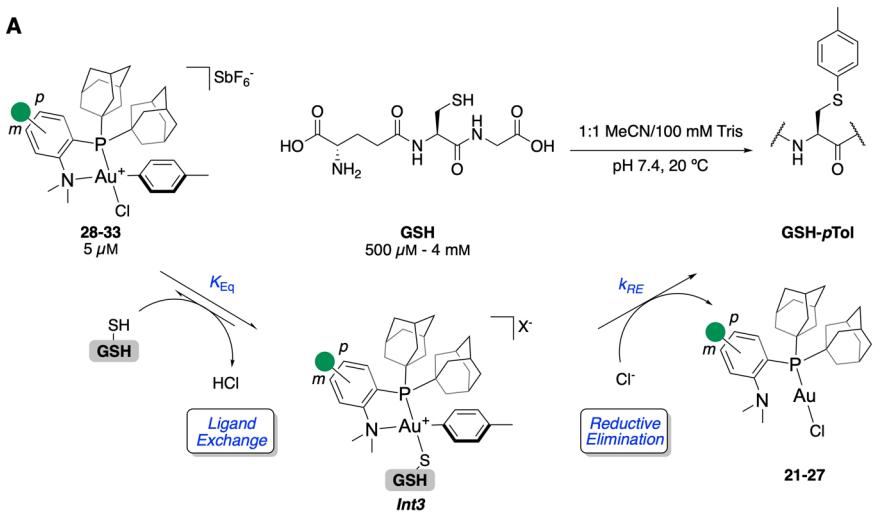

Aryl Substituent	K_{Eq} (M^{-1})	k_{RE} (s^{-1})
H[a]	306	7.92
p-Me (**28**)	291	4.52
p-OMe (**29**)	341	4.24
p-NMe_2 (**30**)	546	2.40
m-Me (**31**)	708	2.61
m-OMe (**32**)	277	4.93
m-NMe_2 (**33**)	N/A	N/A

Figure 4. A) Reaction mechanism for the Au(III)-mediated *S*-arylation of **GSH** from reagents **28**−**33**. X is ambiguous due to counterions in the reaction buffer. B) K_{Eq} and k_{RE} are obtained from stopped-flow/UV−vis spectroscopy rate measurements. See the SI for details. N/A = not applicable due to insolubility of **33** in the reaction conditions. [a]Values determined previously.[24] C) TS_{RE} for the Au(III)-mediated *S*-arylation of **GSH**. X is ambiguous due to counterions in the reaction buffer.

4 weeks on the bench, emphasizing the relatively electron-rich diphosphine on this scaffold. These *P,N*-ligands were then metalated using $HAuCl_4{\cdot}3H_2O$ and 2,2′-thiodiethanol to afford Au(I) complexes **22**−**27** as white solids in 70−95% yield (Figure 3C, see the SI for details). The *P,N*-ligated Au(III) *para*-toluene OACs **28**−**33** were prepared using stoichiometric Au(I) and $AgSbF_6$ with excess *para*-iodotoluene. These Au(III) OACs were synthesized in 68−94% yield and are all bench-stable solids that can be stored outside of the glovebox with no additional precautions (Figure 3D, see the SI for details). These complexes are isolated with the chloride ligand coordinated to Au(III), likely due to the lower solubility of AgI.

To characterize the reactivity of the OACs in the ligand exchange and reductive elimination, Au(III)-mediated *S*-arylation was performed with glutathione (**GSH**) as a model reaction. Stopped-flow/UV−vis spectroscopy was used to profile both the ligand exchange equilibrium and the rate of reductive elimination (Figure 4A). Rate measurements were performed for each of these complexes using a 5 μM solution of the Au(III) reagent with superstoichiometric **GSH** to induce pseudo-first-order conditions (see the SI for details). Complex **33** was not soluble under these conditions and therefore was unsuitable for the kinetics experiments. All of the equilibrium constants (K_{Eq}) for the rapid ligand exchange elementary step for **28**−**32** favor the formation of the *S*-coordinated

https://doi.org/10.1021/acs.orglett.4c04045
Org. Lett. 2024, 26, 10875−10879

intermediate (*Int3*) with values from 277 to 708 M^{-1} (Figure 4B). Reductive elimination from *Int3* via TS_{RE} (Figure 4C) generates the *S*-arylated product (**GSH-*p*Tol**) and the Au(I) byproduct. For the *p*-substituted Au(III) OACs, there is a minimal difference in the reductive elimination rate constant (k_{RE}) for both the methyl (**28**) and methoxy (**29**) substituents at 4.52 and 4.24 s^{-1}, respectively. With the *p*-dimethylamino Au(III) OAC (**30**), there is a notable decrease in the k_{RE} value to 2.40 s^{-1}. Examining the *m*-substituted Au(III) OACs, k_{RE} values of 2.61 s^{-1} for the methyl substituent (**31**) and 4.93 s^{-1} for the methoxy substituent (**32**) were determined (Figure 4B). These results indicate that more electron-rich ligands influence the corresponding Au(III) complexes to undergo slower reductive elimination, with the *p*-dimethylamino (**30**)- and *m*-methyl (**31**)-substituted *P,N*-ligands having the lowest k_{RE} values. Also, the slower rates of reductive elimination for these ligands agree with the observation that the reverse reaction (i.e., oxidative addition) was accelerated with these substituents (Figure 2). As such, we propose that k_{RE} for the *m*-dimethylamino Au(III) OAC (**33**) would be the lowest among the *P,N*-ligated Au(III) OACs tested herein. Additionally, the computed free energy of reductive elimination ($\Delta G_{RE}^{\ddagger}$) of methanethiol from **33** is 1.3 kcal/mol higher in energy than the calculated unsubstituted aryl complex (see the SI for details).[24] The results presented herein are in general agreement with previously calculated Au(I)/Au(III) systems[3,4,11] as well as Pd(0)/Pd(II) systems that can modulate the rates of oxidative addition and reductive elimination based on the electronic properties of the ligand.[34,35]

In this report, both the steric and electronic effects of the *P,N*-ligated compounds were elucidated for the oxidative addition from Au(I) compounds. Using this mechanistic insight, six new electron-rich *P,N*-ligands were synthesized, four of which are synthesized in two steps from commercially available starting materials. The corresponding *P,N*-ligated Au(I) complexes and organometallic Au(III) OACs were isolated. Finally, stopped-flow kinetic analysis was performed on five of these Au(III) OACs to examine the ligand exchange equilibrium and the rates of reductive elimination.[36] Taken together, this work provides key understanding of the elementary steps of *P,N*-ligated Au(I)/Au(III) redox reactions and may allow for the tailoring of ligands to effectively perform Au(I)/Au(III)-catalyzed[37] or -mediated reactions.

■ ASSOCIATED CONTENT

Data Availability Statement

The data underlying this study are available in the published article and its Supporting Information.

Supporting Information

The Supporting Information is available free of charge at https://pubs.acs.org/doi/10.1021/acs.orglett.4c04045.

Experimental details, NMR spectra, characterization, kinetic data, and computational data (PDF)

■ AUTHOR INFORMATION

Corresponding Authors

K. N. Houk − *Department of Chemistry and Biochemistry and California NanoSystems Institute, University of California, Los Angeles, California 90095-1569, United States;* orcid.org/0000-0002-8387-5261; Email: houk@chem.ucla.edu

Heather D. Maynard − *Department of Chemistry and Biochemistry and California NanoSystems Institute, University of California, Los Angeles, California 90095-1569, United States;* orcid.org/0000-0003-3692-6289; Email: maynard@chem.ucla.edu

Alexander M. Spokoyny − *Department of Chemistry and Biochemistry and California NanoSystems Institute, University of California, Los Angeles, California 90095-1569, United States;* orcid.org/0000-0002-5683-6240; Email: spokoyny@chem.ucla.edu

Authors

Joseph W. Treacy − *Department of Chemistry and Biochemistry and California NanoSystems Institute, University of California, Los Angeles, California 90095-1569, United States;* orcid.org/0000-0002-8597-0246

Elaine Y. Chao − *Department of Chemistry and Biochemistry and California NanoSystems Institute, University of California, Los Angeles, California 90095-1569, United States;* orcid.org/0000-0001-6875-718X

Grace E. Kunkel − *Department of Chemistry and Biochemistry and California NanoSystems Institute, University of California, Los Angeles, California 90095-1569, United States;* orcid.org/0000-0001-8137-7552

Thomas Louis-Goff − *Department of Chemistry and Biochemistry and California NanoSystems Institute, University of California, Los Angeles, California 90095-1569, United States;* orcid.org/0009-0004-7572-5302

James A. R. Tilden − *Department of Chemistry and Biochemistry and California NanoSystems Institute, University of California, Los Angeles, California 90095-1569, United States;* orcid.org/0000-0002-4350-2954

Complete contact information is available at: https://pubs.acs.org/10.1021/acs.orglett.4c04045

Author Contributions

The manuscript was written by J. W.T. with contributions from all authors. All authors have given approval to the final version of the manuscript.

Author Contributions

‡J.W.T. and E.Y.C. contributed equally.

Notes

The authors declare the following competing financial interest(s): A.M.S. and H.D.M. are co-inventors on several patent applications from UCLA associated with the Au(III)-based bioconjugation technology.

■ ACKNOWLEDGMENTS

This work was funded in part by the NSF (CHE-2404202, CHE-2003946, and CHE-2153972). A.M.S. thanks NIGMS (R35GM124746) for funding. J.W.T. and G.E.K. thank UCLA's Dissertation Year Fellowship for support. G.E.K. was supported by the NIH under award number T32GM008496. NMR spectrometers are supported in part by the S10 program of the NIH Office of Research Infrastructure Programs under grant S10OD028644. The stopped-flow/UV−vis spectrometer was supported by the NIH (1S10OD023584). This work used computational and storage services associated with the Hoffman2 Shared Cluster provided by the UCLA Institute for Digital Research and Education's Research Technology Group.

REFERENCES

(1) Bratsch, S. G. Standard Electrode Potentials and Temperature Coefficients in Water at 298.15 K. *J. Phys. Chem. Ref. Data* **1989**, *18* (1), 1−21.

(2) Joost, M.; Zeineddine, A.; Estévez, L.; Mallet−Ladeira, S.; Miqueu, K.; Amgoune, A.; Bourissou, D. Facile Oxidative Addition of Aryl Iodides to Gold(I) by Ligand Design: Bending Turns on Reactivity. *J. Am. Chem. Soc.* **2014**, *136* (42), 14654−14657.

(3) Zeineddine, A.; Estévez, L.; Mallet-Ladeira, S.; Miqueu, K.; Amgoune, A.; Bourissou, D. Rational Development of Catalytic Au(I)/Au(III) Arylation Involving Mild Oxidative Addition of Aryl Halides. *Nat. Commun.* **2017**, *8* (1), 565.

(4) Muratov, K.; Zaripov, E.; Berezovski, M. V.; Gagosz, F. DFT-Enabled Development of Hemilabile (P^N) Ligands for Gold(I/III) RedOx Catalysis: Application to the Thiotosylation of Aryl Iodides. *J. Am. Chem. Soc.* **2024**, *146* (6), 3660−3674.

(5) Akram, M. O.; Banerjee, S.; Saswade, S. S.; Bedi, V.; Patil, N. T. Oxidant-Free Oxidative Gold Catalysis: The New Paradigm in Cross-Coupling Reactions. *Chem. Commun.* **2018**, *54* (79), 11069−11083.

(6) McCallum, T. Heart of Gold: Enabling Ligands for Oxidative Addition of Haloorganics in Au(I)/Au(III) Catalysed Cross-Coupling Reactions. *Org. Biomol. Chem.* **2023**, *21* (8), 1629−1646.

(7) Font, P.; Valdés, H.; Ribas, X. Consolidation of the Oxidant-Free Au(I)/Au(III) Catalysis Enabled by the Hemilabile Ligand Strategy. *Angew. Chem. Int. Ed* **2024**, *63* (27), No. e202405824.

(8) Gao, P.; Xu, J.; Zhou, T.; Liu, Y.; Bisz, E.; Dziuk, B.; Lalancette, R.; Szostak, R.; Zhang, D.; Szostak, M. L-Shaped Heterobidentate Imidazo[1,5-*a*]Pyridin-3-ylidene (N,C)-Ligands for Oxidant-Free Au^{I}/Au^{III} Catalysis. *Angew. Chem. Int. Ed* **2023**, *62* (12), No. e202218427.

(9) Scott, S. C.; Cadge, J. A.; Boden, G. K.; Bower, J. F.; Russell, C. A. A Hemilabile NHC-Gold Complex and Its Application to the Redox Neutral 1,2-Oxyarylation of Feedstock Alkenes. *Angew. Chem. Int. Ed* **2023**, *62* (23), No. e202301526.

(10) Harper, M. J.; Arthur, C. J.; Crosby, J.; Emmett, E. J.; Falconer, R. L.; Fensham-Smith, A. J.; Gates, P. J.; Leman, T.; McGrady, J. E.; Bower, J. F.; Russell, C. A. Oxidative Addition, Transmetalation, and Reductive Elimination at a 2,2′-Bipyridyl-Ligated Gold Center. *J. Am. Chem. Soc.* **2018**, *140* (12), 4440−4445.

(11) Cadge, J. A.; Bower, J. F.; Russell, C. A. A Systematic Study of the Effects of Complex Structure on Aryl Iodide Oxidative Addition at Bipyridyl-Ligated Gold(I) Centers. *Angew. Chem. Int. Ed* **2021**, *60* (47), 24976−24983.

(12) Bhoyare, V. W.; Sosa Carrizo, E. D.; Chintawar, C. C.; Gandon, V.; Patil, N. T. Gold-Catalyzed Heck Reaction. *J. Am. Chem. Soc.* **2023**, *145* (16), 8810−8816.

(13) Budzelaar, P. H. M.; Bochmann, M.; Landrini, M.; Rocchigiani, L. Gold-Catalysed Heck Reaction: Fact or Fiction? Correspondence on "Unlocking the Chain Walking Process in Gold Catalysis. *Angew. Chem. Int. Ed* **2024**, *63*, No. e202317774.

(14) Akram, M. O.; Das, A.; Chakrabarty, I.; Patil, N. T. Ligand-Enabled Gold-Catalyzed $C(sp^2)$−N Cross-Coupling Reactions of Aryl Iodides with Amines. *Org. Lett.* **2019**, *21* (19), 8101−8105.

(15) Rodriguez, J.; Adet, N.; Saffon-Merceron, N.; Bourissou, D. Au(I)/Au(III)-Catalyzed C−N Coupling. *Chem. Commun.* **2020**, *56* (1), 94−97.

(16) Liu, H.; Xu, B. Gold-Catalyzed C−N Cross-Coupling Reactions of Aryl Iodides with Alkyl Nitriles or Silver Cyanate. *Org. Lett.* **2024**, *26* (26), 5430−5435.

(17) Das, A.; Patil, N. T. Ligand-Enabled Gold-Catalyzed $C(sp^2)$−O Cross-Coupling Reactions. *ACS Catal.* **2023**, *13* (6), 3847−3853.

(18) Chen, G.; Xu, B. Hydrogen Bond Donor and Unbalanced Ion Pair Promoter-Assisted Gold-Catalyzed Carbon−Oxygen Cross-Coupling of (Hetero)Aryl Iodides with Alcohols. *ACS Catal.* **2023**, *13* (3), 1823−1829.

(19) Mudshinge, S. R.; Yang, Y.; Xu, B.; Hammond, G. B.; Lu, Z. Gold (I/III)-Catalyzed Trifluoromethylthiolation and Trifluoromethylselenolation of Organohalides. *Angew. Chem. Int. Ed* **2022**, *61* (12), No. e202115687.

(20) Urvashi; Mishra, S.; Patil, N. T. Gold-Catalyzed Alkenylation and Arylation of Phosphorothioates. *Chem. Sci.* **2023**, *14* (45), 13134−13139.

(21) Du, W.; Zhao, F.; Yang, R.; Xia, Z. Gold-Catalyzed $C(sp^3)$−$C(sp^2)$ Suzuki−Miyaura Coupling Reaction. *Org. Lett.* **2024**, *26* (15), 3145−3150.

(22) Ye, X.; Wang, C.; Zhang, S.; Tang, Q.; Wojtas, L.; Li, M.; Shi, X. Chiral Hemilabile P,N-Ligand-Assisted Gold Redox Catalysis for Enantioselective Alkene Aminoarylation. *Chem.—Eur. J.* **2022**, *28* (34), No. e202201018.

(23) Chintawar, C. C.; Bhoyare, V. W.; Mane, M. V.; Patil, N. T. Enantioselective Au(I)/Au(III) Redox Catalysis Enabled by Chiral (P,N)-Ligands. *J. Am. Chem. Soc.* **2022**, *144* (16), 7089−7095.

(24) Doud, E. A.; Tilden, J. A. R.; Treacy, J. W.; Chao, E. Y.; Montgomery, H. R.; Kunkel, G. E.; Olivares, E. J.; Adhami, N.; Kerr, T. A.; Chen, Y.; Rheingold, A. L.; Loo, J. A.; Frost, C. G.; Houk, K. N.; Maynard, H. D.; Spokoyny, A. M. Ultrafast Au(III)-Mediated Arylation of Cysteine. *J. Am. Chem. Soc.* **2024**, *146* (18), 12365−12374.

(25) Hesp, K. D.; Stradiotto, M. Stereo- and Regioselective Gold-Catalyzed Hydroamination of Internal Alkynes with Dialkylamines. *J. Am. Chem. Soc.* **2010**, *132* (51), 18026−18029.

(26) Lundgren, R.; Hesp, K.; Stradiotto, M. Design of New 'DalPhos' P,N-Ligands: Applications in Transition-Metal Catalysis. *Synlett* **2011**, *2011* (17), 2443−2458.

(27) Tardiff, B. J.; McDonald, R.; Ferguson, M. J.; Stradiotto, M. Rational and Predictable Chemoselective Synthesis of Oligoamines via Buchwald−Hartwig Amination of (Hetero)Aryl Chlorides Employing Mor-DalPhos. *J. Org. Chem.* **2012**, *77* (2), 1056−1071.

(28) Alsabeh, P. G.; Lundgren, R. J.; McDonald, R.; Johansson Seechurn, C. C. C.; Colacot, T. J.; Stradiotto, M. An Examination of the Palladium/Mor-DalPhos Catalyst System in the Context of Selective Ammonia Monoarylation at Room Temperature. *Chem.—Eur. J.* **2013**, *19* (6), 2131−2141.

(29) Crawford, S. M.; Wheaton, C. A.; Mishra, V.; Stradiotto, M. Probing the Effect of Donor-Fragment Substitution in Mor-DalPhos on Palladium-Catalyzed C−N and C−C Cross-Coupling Reactivity. *Can. J. Chem.* **2018**, *96* (6), 578−586.

(30) MacLean, M. A.; Wheaton, C. A.; Stradiotto, M. Developing Backbone-Modified Mor-DalPhos Ligand Variants for Use in Palladium-Catalyzed C−N and C−C Cross-Coupling. *Can. J. Chem.* **2018**, *96* (7), 712−721.

(31) Ammer, J.; Baidya, M.; Kobayashi, S.; Mayr, H. Nucleophilic Reactivities of Tertiary Alkylamines. *J. Phys. Org. Chem.* **2010**, *23* (11), 1029−1035.

(32) Nigst, T. A.; Antipova, A.; Mayr, H. Nucleophilic Reactivities of Hydrazines and Amines: The Futile Search for the α-Effect in Hydrazine Reactivities. *J. Org. Chem.* **2012**, *77* (18), 8142−8155.

(33) Hansch, C.; Leo, A.; Taft, R. W. A Survey of Hammett Substituent Constants and Resonance and Field Parameters. *Chem. Rev.* **1991**, *91* (2), 165−195.

(34) Martin, R.; Buchwald, S. L. Palladium-Catalyzed Suzuki−Miyaura Cross-Coupling Reactions Employing Dialkylbiaryl Phosphine Ligands. *Acc. Chem. Res.* **2008**, *41* (11), 1461−1473.

(35) Hartwig, J. F. Electronic Effects on Reductive Elimination To Form Carbon−Carbon and Carbon−Heteroatom Bonds from Palladium(II) Complexes. *Inorg. Chem.* **2007**, *46* (6), 1936−1947.

(36) Treacy, J. W.; Chao, E. Y.; Kunkel, G. E.; Louis-Goff, T.; Tilden, J. A. R.; Spokoyny, A. M.; Maynard, H. D.; Houk, K. N. Electronic Effects of Bidentate P,N-Ligands on the Elementary Steps of Au(I)/Au(III) Reactions Relevant to Cross-Coupling Chemistry. *ChemRxiv* 2024, DOI: 10.26434/chemrxiv-2024-7f11b.

(37) Urvashi; Rai, S.; Shukla, G.; Nisha; Patil, N. T. Exploring the Electronic and Steric Effects of Hemilabile (P̂N) Ligands in Redox Gold Catalysis: Application to the Cross-Coupling of Aliphatic Amines with Aryl Iodides. *ChemRxiv* 2024, DOI: 10.26434/chemrxiv-2024-0rwwl.

https://doi.org/10.1021/acs.orglett.4c04045
Org. Lett. 2024, 26, 10875−10879